

# Astragaloside regulates lncRNA LOC100912373 and the miR-17-5p/PDK1 axis to inhibit the proliferation of fibroblast-like synoviocytes in rats with rheumatoid arthritis

HUI JIANG<sup>1,2</sup>, CHANG FAN<sup>1,2</sup>, YUNQI LU<sup>3</sup>, XIAOYA CUI<sup>1,2</sup> and JIAN LIU<sup>1</sup>

<sup>1</sup>Experimental Center of Clinical Research, The First Affiliated Hospital of Anhui University of Chinese Medicine, Hefei, Anhui 230031; <sup>2</sup>School of Pharmacy, Anhui University of Chinese Medicine, Hefei, Anhui 230012, P.R. China; <sup>3</sup>Department of Biochemistry, Drew University, Madison, NJ 07940, USA

Received January 20, 2021; Accepted April 26, 2021

DOI: 10.3892/ijmm.2021.4963

**Abstract.** Previous studies have confirmed that astragaloside (AST) exerts a positive effect on alleviating synovial and joint injury in rheumatoid arthritis (RA). However, the precise mechanisms through which AST acts in the treatment of RA remain unclear. Long non-coding RNA (lncRNA) LOC100912373 was identified as a key gene related to RA and has been proven to interact with miR-17-5p, in order to regulate the pyruvate dehydrogenase kinase 1 and protein kinase B axis (PDK1/AKT axis). The present study aimed to determine whether AST may treat RA through the interaction between lncRNA LOC100912373 and the miR-17-5p/PDK1 axis. MTT assays and flow cytometry were used to detect the proliferation and cell cycle progression of AST-treated fibroblast-like synoviocytes (FLSs). The expression of lncRNA LOC100912373 and miR-17-5p, as well as relative the mRNA expression of the PDK1 and AKT genes following AST intervention was detected by reverse transcription-quantitative PCR (RT-qPCR), immunofluorescence and western blot analysis. The results revealed that AST inhibited FLS proliferation, reduced lncRNA LOC100912373 expression levels, increased miR-17-5p expression levels, and decreased the PDK1 and p-AKT expression levels. Additionally, consecutive rescue experiments revealed that AST counteracted the effects of lncRNA LOC100912373 overexpression on FLS proliferation and cell cycle progression. On the whole, the present study demonstrates that AST inhibits FLS proliferation by regulating the expression of lncRNA LOC100912373 and the miR-17-5p/PDK1 axis.

## Introduction

Rheumatoid arthritis (RA), a chronic multisystem disease associated with autoimmunity, is typically characterized by the excessive proliferation of synovial cells (1,2). The global incidence of RA is approximately 0.5 to 1.0%, and the incidence among the female population is significantly higher than among the male population (3,4). Without timely diagnosis and treatment, RA may further lead to joint damage and disability, severely affecting health and the quality of life of patients (5,6). Fibroblast-like synoviocytes (FLSs) are the stromal cells of the joint capsule and play important roles in the development of RA (7). The abnormal activation and proliferation of FLSs can cause damage to the joint synovium and accelerate the disease progression of RA (8). According to existing research, the pathogenesis of RA is related to a number of factors; however, the specific etiology remains unclear (9,10). At present, the most common clinical treatment for RA mainly includes the treatment of symptoms to reduce pain experienced by patients; however, the effects of these treatments are not ideal, and they often lead to certain side-effects. Therefore, the development of novel treatment strategies for RA is of utmost importance.

Traditional Chinese medicine has been applied as a means of RA treatment for thousands of years; some of these medicines are still used frequently and have been proven effective (11,12). Huang Qi (*Astragalus membranaceus*), one of the most common traditional Chinese medicinal herbs, bearing a long history of medicinal use, has been observed to be therapeutically effective in the course of RA and its related complications. For example, Liu *et al* (13) found that the total flavonoids of *Astragalus membranaceus* reduced adjuvant arthritis-associated damage in rats by regulating the OPG/RANKL/NF- $\kappa$ B pathway. Pu *et al* (14) proved that *Astragalus membranaceus* polysaccharides exerted therapeutic effects on inflammation and synovial cell apoptosis in rats with adjuvant arthritis. Astragaloside (AST) is the main active ingredient of Huang Qi, including Astragaloside I-VIII. AST has been shown to exert antioxidative, anti-inflammatory, and immune regulatory effects (15-17). In a previous study by the authors, it was found that AST alleviated RA-associated

---

*Correspondence to:* Dr Jian Liu, Experimental Center of Clinical Research, The First Affiliated Hospital of Anhui University of Chinese Medicine, 117 Meishan Road, Hefei, Anhui 230031, P.R. China  
E-mail: liujianahzy@ahtcm.edu.cn

**Key words:** astragaloside, rheumatoid arthritis, fibroblast-like synoviocytes, lncRNA LOC100912373, miR-17-5p/PDK1 axis

pathological injury and regulated long non-coding RNA (lncRNA) abnormal expression (18).

An increasing number of studies have shown that lncRNAs, which are >200 nucleotide (nt) in length and lack an open reading frame, play important roles in a variety of biological processes and participate in the pathogenesis of a number of autoimmune diseases (19,20). As the authors have previously demonstrated, lncRNAs with a differential expression in RA can regulate microRNAs (miRNAs or miRs), as competitive endogenous RNAs (ceRNAs) and can subsequently affect RA occurrence and development (21). Moreover, as also previously demonstrated by Bi *et al* (22), lncRNA PICSAR promoted the proliferation, migration and invasion of FLSs by sponging miRNA-4701-5p in RA. Therefore, with lncRNAs and miRNAs as the starting point, research on novel therapeutic targets of RA may prove helpful for identifying new clinical diagnosis and treatment strategies.

In a previous study by the authors, it was demonstrated that lncRNA LOC100912373 was critical for RA pathogenesis (23). In subsequent studies, was further validated that lncRNA LOC100912373 upregulated the expression of 3-phosphoinositide-dependent protein kinase-1 (PDK1) by sponging miR-17-5p, and thus enhancing FLS proliferation (24). In the present study, the effects of AST on FLS proliferation and cell cycle progression, and on lncRNA LOC100912373/miR-17-5p/PDK1 axis component expression levels were investigated and the mechanisms through which AST functions in the treatment of RA were elucidated.

## Materials and methods

**Materials and reagents.** AST was purchased from Zhibaicui Biotechnology Co., Ltd., and its purity was >98.5%. Complete Freund's adjuvant was purchased from Sigma-Aldrich; Merck KGaA. DMEM was purchased from Gibco; Thermo Fisher Scientific, Inc. Anti-Vimentin antibody (cat. no. ab92547) was purchased from Abcam. PI staining solution was purchased from Beijing Solarbio Science & Technology Co. An MTT assay kit was purchased from Shanghai, BestBio. EZ-10 Total RNA Mini-Preps kit reagent was purchased from Sangon Biotech Co., Ltd. A reverse transcription kit was obtained from ABclonal Biotech Co., Ltd. Antibodies against PDK1 (cat. no. ab110025), AKT (cat. no. ab18785) and phosphorylated (p-)AKT (cat. no. ab38449) were purchased from Abcam. Secondary antibodies (anti-mouse or anti-rabbit; cat. nos. ZB-2301 and ZB-2305) were purchased from Beijing ZSGB-BIO. Cy3-labeled goat anti-rabbit antibody (cat. no. A0516) was purchased from Beyotime Institute of Biotechnology. The pcDNA3.1 plasmid was synthesized by Shanghai GenePharma Co., Ltd. Lipofectamine® 2000 Transfection Reagent was purchased from Invitrogen; Thermo Fisher Scientific, Inc.

**Animals.** In the present study, male Sprague-Dawley SPF grade rats (6-8 weeks old, weighing 200±20 g) were purchased from the Experimental Animal Center of Anhui Province. All rats were raised in the animal facility of the First Affiliated Hospital of Anhui University of Chinese Medicine with an indoor temperature of 18-22°C and a humidity of 40-60%,

under 12-h alternate dark/light cycle. Regular rat feed and tap water were provided *ad libitum*. The experimental design was approved by the Animal Ethics Committee of Anhui University of Chinese Medicine (AHUCM-rats-004). Following one week of adaptive feeding, a model of adjuvant arthritis (AA) was established by a single injection of Freund's adjuvant into the left hind foot of the rats, as previously described by Jiang *et al* (25).

**Cell culture and identification.** Following 20 days of AA modeling (25), the rats were anesthetized by an intraperitoneal injection of 1.0% pentobarbital sodium (60 mg/kg body weight) and sacrificed by cervical dislocation after blood sampling from the abdominal aorta. A quantity of 8-10 ml blood volume was collected, and the synovial tissue of the knee joint was then separated, as previously described (26). The animal remains were subsequently sent to the Anhui Experimental Animal Carcass Management Organization for unified processing. The FLSs were cultured in complete DMEM containing 20% fetal bovine serum at 37°C and 5% CO<sub>2</sub> through tissue mass culture method (27). At different time points, the FLSs were evaluated under an inverted phase contrast microscope (Olympus Corporation), and passaged synoviocytes were identified by vimentin immunofluorescence staining. The standard method of immunofluorescence staining was then applied as described below.

**MTT assay.** The cells were digested with trypsin and seeded in a 96-well plate (5,000 cells per well). AST was diluted in culture medium to a desired concentration (7.8125, 15.625, 31.25, 62.5, 125, 250 and 500 mg/l), added to the cells and then incubated for 24, 48 and 72 h at 37°C. Subsequently, 10 µl MTT were added 4 h before the end of culture. Following 4 h of continuous culture, 100 µl formazan solution were added to each well, and the plates were oscillated at a low speed for 10 min, in order to fully dissolve the crystals. The 96-well plates were removed when all the purple crystals were dissolved. The optical density was measured using a microplate reader (Multiskan™ GO; Thermo Fisher Scientific, Inc.) at 570 nm (28).

The IC<sub>50</sub> values were also calculated according to the following formula:  $\lg IC_{50} = X_m - I [P - (3 - P_m - P_n) / 4]$ , where  $X_m$  represents the lg maximum dose;  $I$  represents the lg (maximum dose/relative dose);  $P$  represents the sum of the positive reaction rate;  $P_m$  represents the maximum positive reaction rate; and  $P_n$  represents the minimum positive reaction rate. Inhibition rate =  $(1 - OD_{\text{experimental group}} / OD_{\text{control group}}) \times 100$ .

**Cell cycle assay.** The cells were cultured with AST (50 mg/ml), and were then collected at the point when a density of  $1 \times 10^6$  cells/ml was reached. Subsequently, 100 µg/ml PI staining solution (100 ml) were added, followed by a 30-min incubation in the dark. The percentage of synovial cells in each stage was detected by flow cytometry (Beckman Coulter, Inc.), in order to observe the effect of AST on FLS cell cycle progression.

**Cell ultrastructure.** Cells treated with AST were collected, fixed with 2.5% glutaraldehyde and 1% ozone acid, dehydrated with acetone and infused with an epoxy resin embedding

agent. Finally, the samples were sectioned and stained, and the ultrastructure of the cells was observed through transmission electron microscopy (Hitachi, Ltd.).

**Reverse transcription-quantitative PCR (RT-qPCR).** Total RNA was extracted from the FLSs using an EZ-10 Total RNA Mini-Preps kit, and RNA was then reverse transcribed into cDNA with the use of a reverse transcription kit. PCR analyses were performed with TB Green™ Premix Ex Taq™ II (Takara Bio, Inc.). The reaction conditions were as follows: Pre-denaturation at 95°C for 30 sec, 40 cycles at 95°C for 5 sec and 60°C for 1 min.  $\beta$ -actin was used as the endogenous control. All the results were calculated using the  $2^{-\Delta\Delta C_q}$  method (29) and all primers were synthesized by Shanghai Sangon Biotech Technology Service Co., Ltd. Primer sequences are listed in Table SI.

**Western blot analysis.** The cells were washed with cold PBS three times and lysed with 100  $\mu$ l lysis buffer. The lysates were then separated by sodium dodecyl sulfate-polyacrylamide gel electrophoresis (SDS-PAGE; concentrated gel, 5%; separating gel, 10%) and then transferred to a polyvinylidene fluoride (PVDF) membrane. The PVDF membrane was washed with 1X TBST for 2 min, blocked with 5% skim milk at room temperature for 2 h, and incubated with a primary anti-PDK1 antibody (1:500), an anti-AKT antibody (1:1,000) and an anti-p-AKT antibody (1:1,000) overnight at 4°C. The cells were then washed three times with TBST and incubated with a secondary HRP-conjugated anti-rabbit antibody HRP (1:10,000) for 2 h at room temperature. All blotting experiments were performed three times. The proteins were detected with an enhanced chemiluminescence kit (Super Signal WestFemto kit; 34094; Thermo Fisher Scientific, Inc.). The western blot analysis data were quantified using ImageJ software (version 1.52; National Institutes of Health).

**Immunofluorescence.** Cells were fixed in 4% paraformaldehyde for 30 min. A total of 50-100  $\mu$ l 0.25% Triton X-100 was added and the sections were incubated for 10 min at room temperature. The sections were washed with PBS three times, primary antibodies were added, and the sections were immunostained overnight in a wet chamber at 4°C (antibody dilutions: PDK1, 1:200; p-AKT, 1:200). All sections were then stained with the corresponding secondary antibody [goat anti-rabbit IgG H&L (FITC); dilution, 1:1,000; cat. no. ab6717, Abcam] and incubated at room temperature for 50 min. In the end, nuclei were stained with DAPI at room temperature for 5 min. Immunofluorescence was observed under a fluorescence microscope (Nikon Corporation).

**Rescue experiment.** To further confirm whether AST interferes with FLS proliferation and cell cycle progression by regulating lncRNA LOC100912373 expression, a rescue experiment was conducted. Full-length lncRNA LOC100912373 was cloned into the pcDNA3.1 plasmid to construct an overexpression plasmid; this construct was labeled lncRNA LOC100912373 overexpression (Over). In addition, the empty pcDNA3.1 vector was labeled as the negative control (NC). The cells were seeded in a 6-well plate in advance, in order to ensure

that cell confluence was 60 to 80% per well at the time of transfection. The lncRNA LOC100912373 overexpression and NC plasmids were transfected into the FLSs using Lipofectamine® 2000. Specific transfection operation and screening of the optimum overexpression concentration of lncRNA LOC100912373 (2.5  $\mu$ g/5  $\mu$ l) were performed according to a published method by the authors (24), and the FLSs were treated with AST (50 mg/ml) simultaneously. At 48 h after transfection, the cells were collected and cell proliferation and cell cycle progression was detected by MTT assay and flow cytometry.

**Statistical analysis.** All data were analyzed using SPSS 17.0 software (SPSS, Inc.), and results are expressed as the mean  $\pm$  SD (standard deviation). One-way analysis of variance (ANOVA) was used for comparisons among multiple groups and Tukey's multiple comparisons test was used to define differences between groups.  $P < 0.05$  was considered to indicate a statistically significant difference.

## Results

**Identification of FLSs.** The morphology of the FLSs was observed under a microscope. Following three days of culture, the primary synovial cells were gradually separated from the edge of the synovial tissue (Fig. 1A). After the primary synovial cells were cultured for 14 days, the synovial tissue mainly disappeared, a large number of synovial cells were dissociated, and the cells were oval and spindle-shaped (Fig. 1B). After undergoing three passages, the synovial cells were uniform and spindle-shaped. Those cells were then used in the follow-up experiment (Fig. 1C). Under a fluorescence microscope, the CY3-labeled cytoplasm appeared red in colour, and the DAPI-labeled nucleus, in blue. As depicted in Fig. 1D-F, all cells were fusiform and homogeneous in shape, which was consistent with standard FLS cell morphology (30).

**Effects of AST on FLS proliferation, cell cycle progression and cell ultrastructure.** As shown in Fig. 2A, the FLS inhibition rate increased further with the increasing AST concentration. On the other hand, in comparison with the inhibition rate at 24 h, the 48- and 72-h inhibition rates were significantly increased in response to the various AST concentrations. However, there was no significant difference between the increase rate at 48 and 72 h. Therefore, the 48-h incubation time was selected for use in follow-up experiments. According to the calculations, the  $IC_{50}$  value of AST at 48 h was 48.59 mg/l; thus, 50 mg/l was selected as the drug concentration for stimulation in the follow-up experiments (Fig. 2B).

As shown in Fig. 2C and D, the model group exhibited significantly decreased numbers of FLSs in the G0/G1 phase, whereas it exhibited significantly increased numbers of FLSs in the G2/M phase, in comparison with the control group. In addition, the AST group exhibited significantly increased numbers of FLSs in the G0/G1 phase, whereas it exhibited significantly decreased numbers of FLSs in the G2/M phase, in comparison with the control group.

Under a transmission electron microscope, the FLSs were evidently fusiform. In the control group, the cell membranes were intact, the nuclei were oval and clearly visible, and a

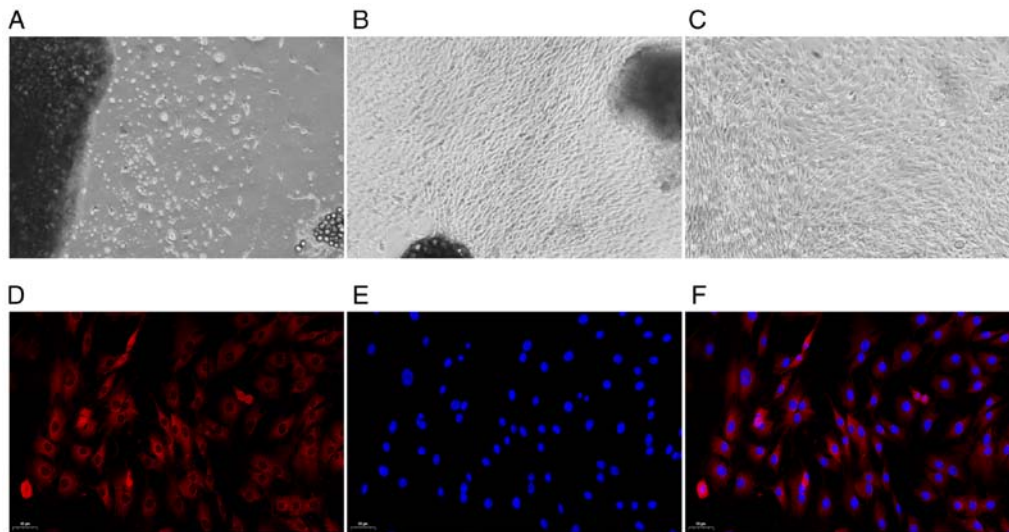


Figure 1. Observation of synovial cell morphology by optical microscopy and fluorescence microscopy (A-C) magnification, x40; (D-F) magnification, x100. (A) Primary culture for three days. (B) Primary culture for 14 days. (C) FLS subculture (three times). (D) Cytoplasmic staining. (E) Nuclear staining. (F) Merged image. FLS, fibroblast-like synoviocyte.

large number of endoplasmic reticulum and mitochondria could be seen in the cytoplasm (Fig. 2E). The model group cell morphology was apparently aberrant compared with that of the control group, and the model group mainly included FLSs that were swollen and had damaged, dilated and incomplete cell membranes. Moreover, the cell nuclear shape was irregular, the nuclear membrane was blurred and the nucleolus could not be clearly distinguished in the model group. Additionally, the endoplasmic reticulum in the cytoplasm was significantly expanded and the number of mitochondria was significantly decreased in the model group, when compared with the control group (Fig. 2F). These changes suggested that the model group FLSs were in an activated state. Following AST treatment, there was an improvement in the above-mentioned pathological phenomena in FLSs (Fig. 2G).

**Effects of AST on FLS lncRNA LOC100912373 and miR-17-5p expression.** As shown in Fig. 3A, the lncRNA LOC100912373 expression levels in the model group were significantly higher in contrast to the control group expression levels. However, the AST group lncRNA LOC100912373 expression levels were significantly lower. As presented in Fig. 3B, compared with the control group, the model group exhibited a significantly decreased miR-17-5p expression. The miR-17-5p expression levels were significantly increased in the AST group, in comparison to the model group expression levels.

**Effect of AST on FLS PDK1 and AKT expression.** PDK1 controls cell growth, differentiation, survival, protein translation and glucose metabolism by activating related protein kinases (31,32). As shown in the Fig. 4A, PDK1 was mainly expressed in the cytoplasm, and PDK1 mRNA and protein expression levels were significantly increased in the model group. Following AST treatment, PDK1 mRNA and protein expression was significantly decreased (Fig. 4B-D).

AKT, a protein kinase that regulates cell survival and apoptosis, is phosphorylated by PDK1 (33,34). As shown in

Fig. 4E, p-AKT was also mainly expressed in the cytoplasm, and there were no significant differences in the mRNA and protein expression of AKT among the three groups. However, when compared with the control group, the model group exhibited a significantly increased mRNA and protein expression of p-AKT. Conversely, following AST treatment, p-AKT mRNA and protein expression was significantly decreased (Fig. 4F-H).

**AST reverses the effects of lncRNA LOC100912373 overexpression on FLSs.** To determine whether the effect of AST on FLSs was achieved by regulating lncRNA LOC100912373 expression, a rescue experiment was performed. As depicted in Fig. 5A, following transfection with overexpression plasmid, the expression levels of lncRNA LOC100912373 were significantly increased according to the corresponding RT-qPCR results, indicating that the plasmid was successfully transfected into the FLSs. As shown in Fig. 5B, the rate of FLS inhibition was significantly decreased following lncRNA LOC100912373 overexpression, in contrast to impact upon the model group FLS inhibition rate. Of note, after AST treatment was applied to the lncRNA LOC100912373 overexpression group, the rate of FLS inhibition was significantly reversed, to some extent.

As shown in Fig. 5C and D, the cell cycle progression results were also consistent with the aforementioned results. The number of FLSs in the G0/G1 phase significantly decreased and the number of FLSs in the G2/M phase significantly increased following the overexpression of lncRNA LOC100912373, while AST intervention restored the effects of lncRNA LOC100912373 overexpression on the FLS cell cycle.

## Discussion

Currently, RA treatments mainly focus on mitigating symptoms and preventing complications rather than reversing or curing RA. The pathogenesis of RA is extremely complex

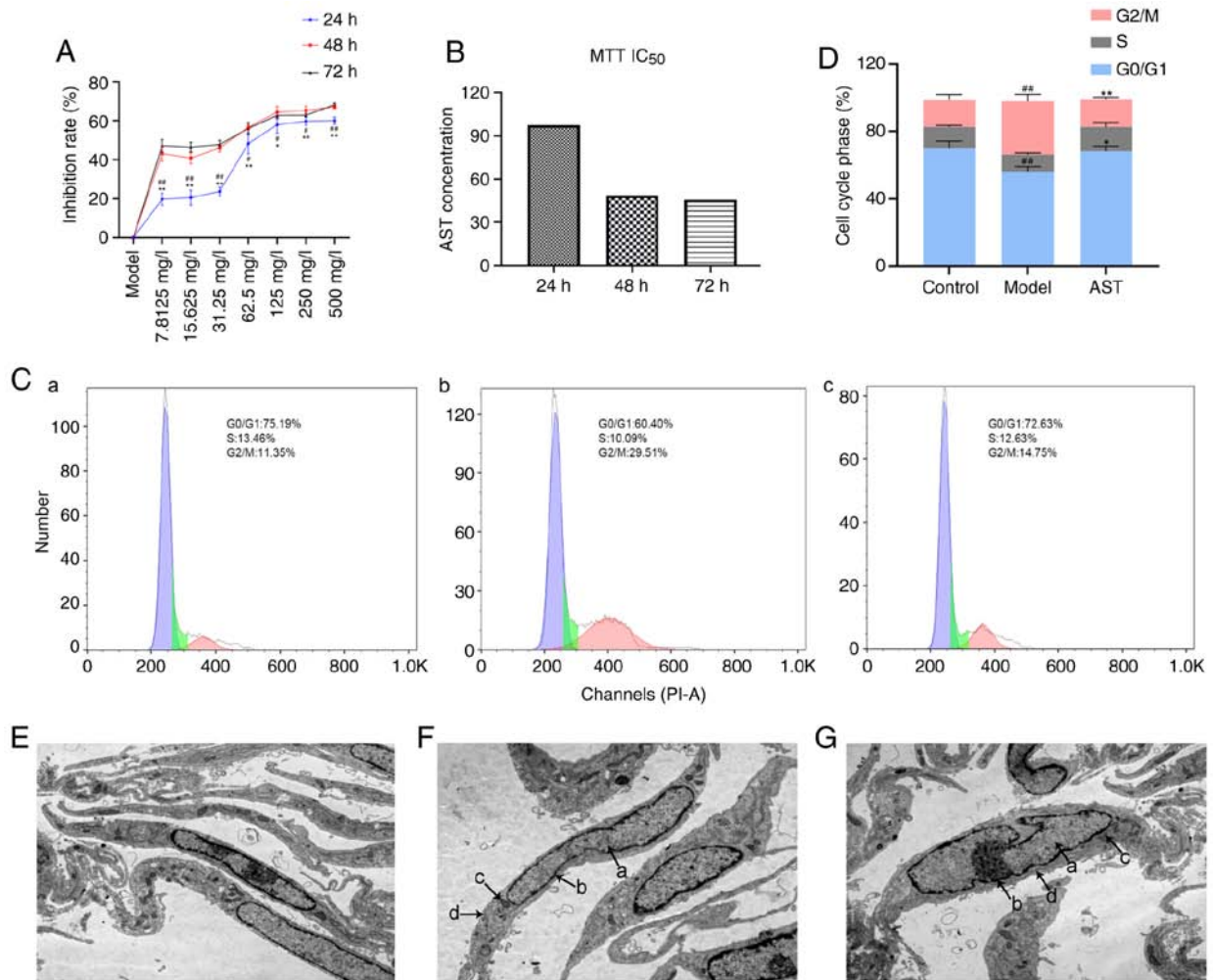


Figure 2. Effect of AST intervention on FLS proliferation, cell cycle progression and cell ultrastructure. (A) Inhibition rate in the groups treated with various concentrations of AST under different reaction times. \* $P < 0.05$  and \*\* $P < 0.01$ , compared with the 72-h intervention; \* $P < 0.05$  and \*\* $P < 0.01$ , compared with the 48-h intervention. (B) IC<sub>50</sub> value calculated by MTT assay. (C) Cell cycle phase was detected by flow cytometry. (a) Control group; (b) model group; (c) AST group. (D) Quantification of the cell cycle results. \*\* $P < 0.01$ , compared with the control group; \*\* $P < 0.01$ , compared with the model group. (E) Control group (magnification,  $\times 12,000$ ). (F) Model group (magnification,  $\times 12,000$ ). (G) AST group (magnification,  $\times 12,000$ ). a, nucleus; b, nuclear membrane; c, mitochondria; d, endoplasmic reticulum; ALS, astragaloside; FLS, fibroblast-like synoviocyte.

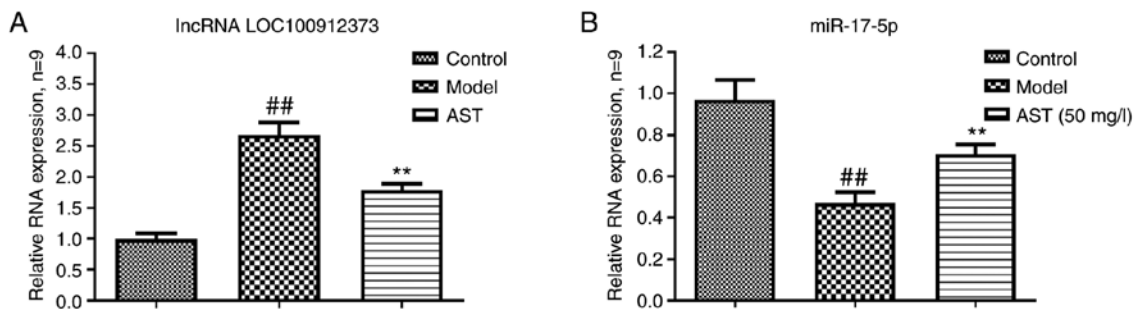


Figure 3. Effect of AST on lncRNA LOC100912373 and miR-17-5p expression. (A) Changes in lncRNA LOC100912373 expression in FLS following AST intervention. (B) Changes in miR-17-5p expression in FLSs following AST intervention. \*\* $P < 0.01$ , compared with the control group; \*\* $P < 0.01$ , compared with the model group. ALS, astragaloside; FLS, fibroblast-like synoviocyte.

and involves environmental, immune, genetic and other factors (35,36), thus rendering the achievement of RA targeted treatment development a difficult research target. Currently, increasing attention has been paid to the role of natural herbal extracts with a probable therapeutic effect on the treatment of several diseases, including RA (37,38). For

example, *Astragalus membranaceus*, *Tripterygium wilfordii* and *Radix Paeoniae Alba* have been proven to have certain therapeutic effects on RA (39-41). The therapeutic effect of traditional Chinese herbs on diseases mainly depends on a variety of active components. For example, AST and other ingredients are components of *Astragalus membranaceus*.

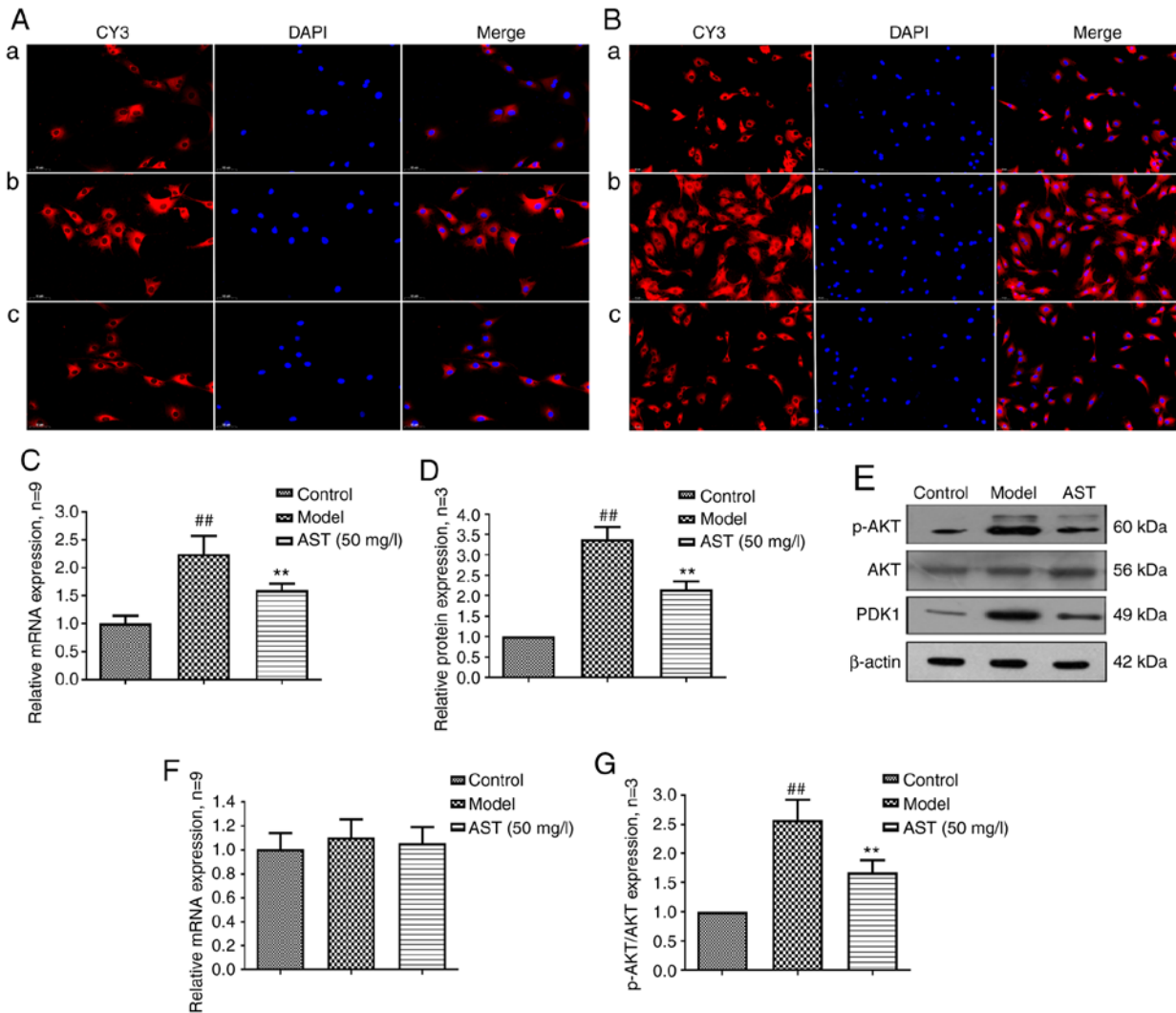


Figure 4. PDK1 and AKT protein and mRNA expression changes in FLSs following AST intervention. (A) PDK1 protein expression changes were observed through immunofluorescence technique (magnification, x200). (a) Control group; (b) model group; (c) AST group. (B) p-AKT protein expression changes were detected through immunofluorescence technique (magnification, x200). (a) Control group; (b) model group; (c) AST group. (C) PDK1 mRNA expression changes were detected through RT-qPCR. (D) Semi-quantitative analysis of PDK1 protein.  $^{##}P<0.01$ , compared with the control group;  $^{**}P<0.01$ , compared with the model group. (E) PDK1, AKT and p-AKT protein expression changes were detected by western blot analysis. (F) AKT mRNA expression changes were detected by RT-qPCR. (G) Semi-quantitative analysis of p-AKT/AKT protein.  $^{##}P<0.01$ , compared with the control group;  $^{**}P<0.01$ , compared with the model group. ALS, astragaloside; FLS, fibroblast-like synoviocyte.

Some studies have proven that AST may exert beneficial therapeutic effects on a variety of diseases, through the modulation of immune function and the inhibition of inflammatory factor production (42,43). In a previously published study by the authors, it was elucidated that AST may exert a regulatory effect on differentially expressed lncRNAs during the development of RA (18). In the present study, the above-mentioned results were further validated, and it was attested that AST regulated the expression of lncRNA LOC100912373, miR-17-5p and PDK1 in the FLSs of rats with AA.

Being a type of RNA that has been linked to cell biological activities, lncRNAs are indispensable cell function regulators. In addition to directly regulating cell function, lncRNAs can also act as ceRNAs, that regulate miRNA and mRNA downstream expression, thus affecting RA disease occurrence and development (44). Zhao *et al* (45) confirmed that lncRNASMAD5-AS1, a ceRNA, inhibits the proliferation of diffuse large B cell lymphoma via the Wnt/ $\beta$ -catenin

pathway by sponging miR-135b-5p to increase the expression of APC. Similarly, lncRNAs are also inextricably linked to RA. In contemporary RA research, lncRNAs have received extensive attention as diagnostic biomarkers and as potential therapeutic targets for RA (46,47). Some studies have proven that lncRNA expression is related to the risk and activity of RA. In addition, lncRNAs can participate in the regulation of relevant signaling pathways in order to affect FLS proliferation (48,49). In a previously published study, it was verified that lncRNA LOC100912373 is a differentially expressed gene that is crucial for the occurrence and development of RA; in addition, lncRNA LOC100912373 can induce FLS proliferation by competing with miR-17-5p, so as to promote PDK1/AKT signaling pathway activation, thereby promoting RA progression (24). Notably, in the present study, it was revealed that AST reduced lncRNA LOC10091237 expression and increased miR-17-5p levels, in order to affect PDK1 axis activation in the FLSs of rats with AA.

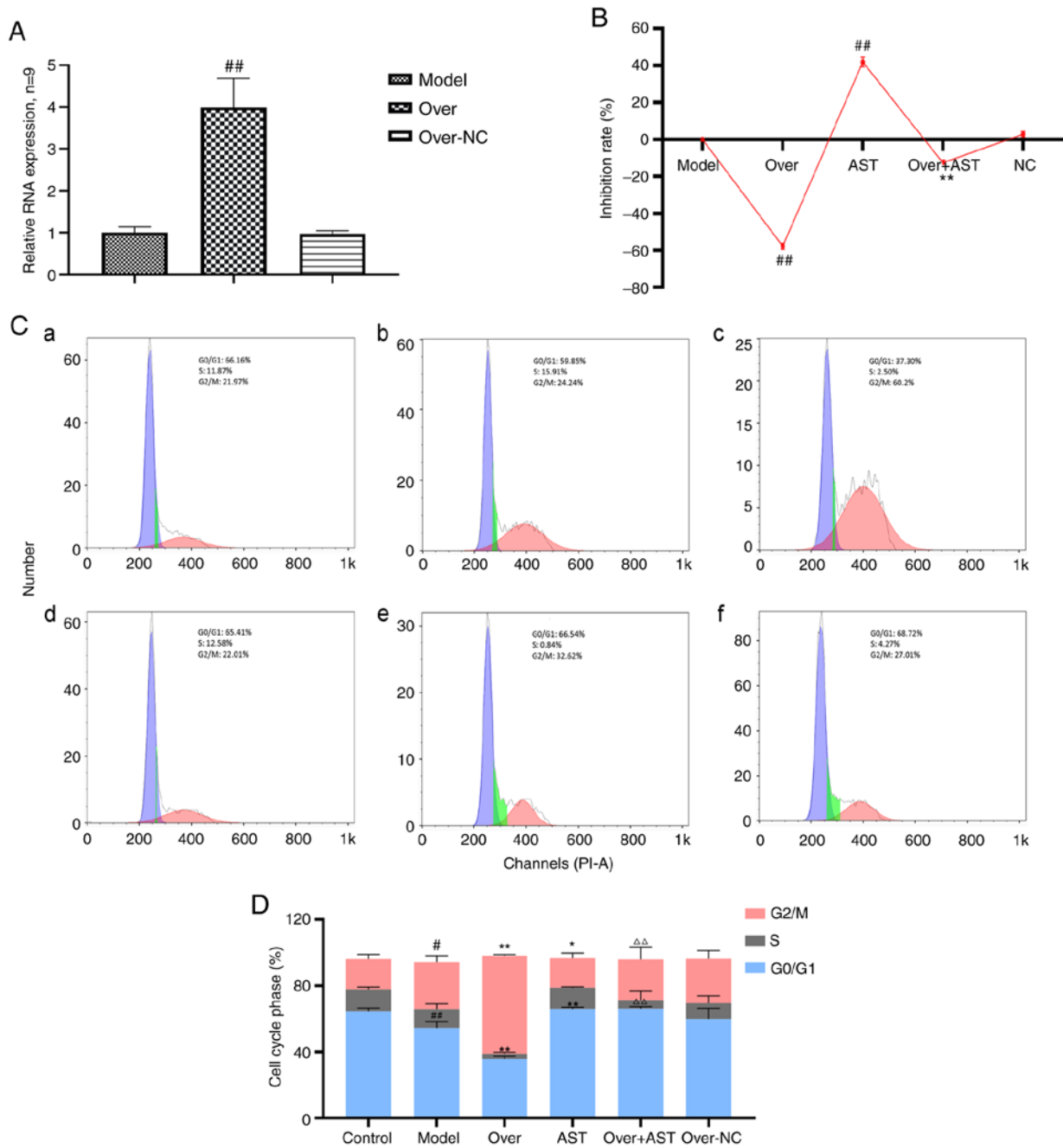


Figure 5. Effect of AST on FLS proliferation and cell cycle with lncRNA LOC100912373 overexpression. (A) lncRNA LOC100912373 expression levels following transfection with overexpression plasmid was detected by RT-qPCR. <sup>##</sup>P<0.01, compared with the model group. (B) FLS inhibition rate between groups, under a 48-h intervention time. <sup>##</sup>P<0.01, compared with the model group; <sup>\*\*</sup>P<0.01, compared with the lncRNA LOC100912373 overexpression group. (C) Cell cycle phase was detected by flow cytometry. (a) Control group; (b) model group; (c) lncRNA LOC100912373 overexpression group; (d) AST group; (e) lncRNA LOC100912373 overexpression and AST intervention group; (f) NC group. (D) Cell cycle phase quantification. <sup>#</sup>P<0.05, compared with the control group; <sup>##</sup>P<0.01, compared with the control group; <sup>\*</sup>P<0.05, compared with the control group; <sup>\*\*</sup>P<0.01, compared with the model group; <sup>△△</sup>P<0.01, compared with the lncRNA LOC100912373 overexpression group. ALS, astragaloside; FLS, fibroblast-like synoviocyte.

PDK1 is a serine/threonine kinase, which belongs to the AGC kinase family. AKT, also known as protein kinase B (PKB), is the downstream target gene of PDK1. Some studies have demonstrated that the PDK1/AKT signaling pathway is involved in the occurrence and development of RA, through the regulation of several cell biological processes, such as cell proliferation, cell cycle progression and differentiation (50,51). More specifically, as an important protein of the PI3K/AKT signaling pathway, PDK1 can bind to the product of activated PI3K, PIP3. Afterwards, PDK1/PIP3 complex transfers to the

cell membrane, in order to phosphorylate AKT and activate AKT signaling pathway (52). AKT signaling pathway activation can accelerate the release of pro-inflammatory factors and thus may lead to abnormal cell biological processes, such as excessive cell proliferation, decrease in cell proliferation and increase in cell necrosis (53,54). In general, it is known that excessive FLS proliferation is an important principal pathological feature of RA. Because cell proliferation is controlled through the regulation of the cell cycle, abnormal cell cycle progression must occur during the development of

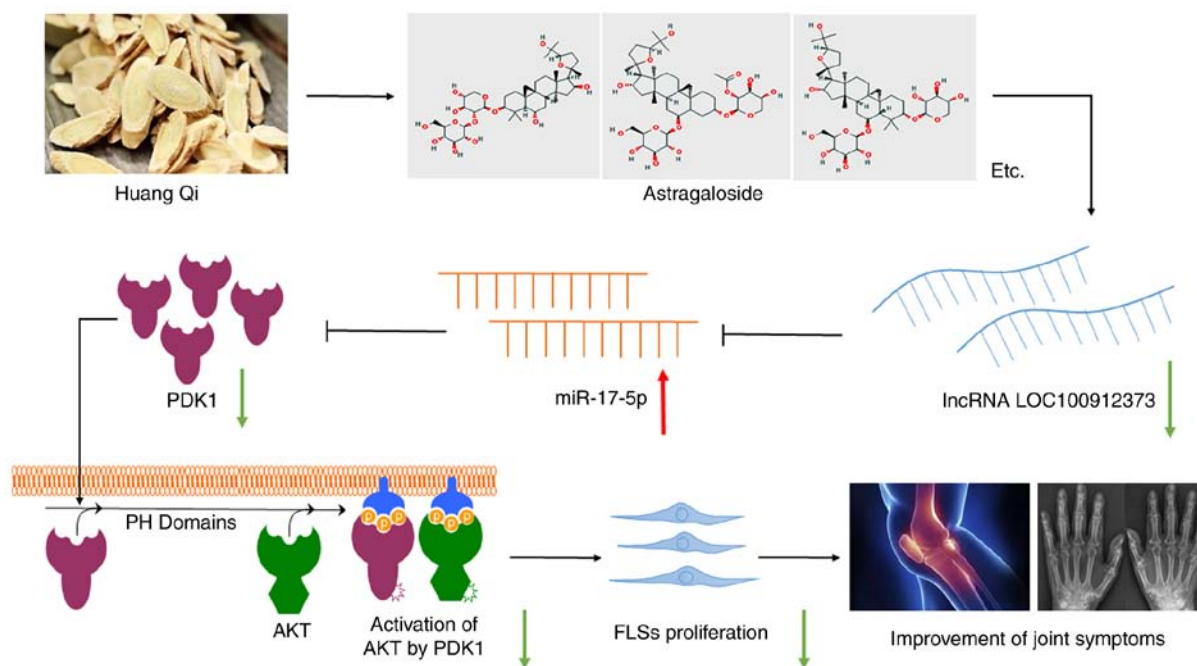


Figure 6. Therapeutic effect of AST on RA is achieved through the inhibition of lncRNA LOC100912373 expression, the increased release of miR-17-5p binding to PDK1, the prevention of PDK1/AKT signaling pathway activation and FLS proliferation reduction. ALS, astragaloside; FLS, fibroblast-like synoviocyte.

RA. In a previously published research by Fu *et al* (55), PDK1 promoted proliferation and inhibited apoptosis in human spermatogonial stem cells via the PDK1/KDR/ZNF367, ERK1/2 and AKT pathway. In the present study, it was demonstrated that AST can suppress excessive proliferation and restore the normal cell cycle progression of the FLSs in AA rats. In addition, PDK1 and p-AKT mRNA and protein expression levels were significantly decreased in FLSs following AST treatment. Moreover, in order to further validate the above-mentioned results, a rescue assay was carried. Thus, it was confirmed that the excessive proliferation and the establishment of abnormal cell cycle progression caused by lncRNA LOC100912373 overexpression in FLSs could be reversed by AST treatment (Fig. 6).

In conclusion, the results of the present study revealed that AST suppressed the excessive proliferation of FLSs in rats with AA, through the inhibition of lncRNA LOC100912373 expression. miR-17-5p binds to PDK1, and thereby prevents PDK1/AKT signaling pathway activation. Therefore, AST may serve as a potential therapeutic for RA, and the results of the present study may provide novel insight into future research for the use of traditional Chinese medicines for the prevention and treatment of RA.

### Acknowledgements

The authors are grateful to Mr. Qiang Fan (Ao Ji Bio-tech Co. Ltd., Shanghai, China) for providing assistance with the data analysis.

### Funding

The present study was supported by the National Natural Science Foundation of China (grant no. 81873139), the 12th

Batch of '115' Innovation Team of Anhui Province [Anhui Talent Office (2019) no. 1], the Key Research and Development Program of Anhui Province, China (no. 201904a07020004) and the Special Funds for Provincial TCM Development (no. 2016ZYZJ01).

### Availability of data and materials

The datasets used and/or analyzed during the present study are available from the corresponding author on reasonable request.

### Authors' contributions

JL made substantial contributions to the conception and design of the study. HJ, CF, YL and XC performed the experiments. HJ and CF contributed to data acquisition, and data analysis and interpretation. HJ revised the manuscript critically for important intellectual content. HJ and JL confirm the authenticity of all the raw data. All authors agreed to be accountable for all aspects of the work in ensuring that questions related to the accuracy or integrity of the work are appropriately investigated and resolved. All authors read and approved the final manuscript.

### Ethics approval and consent to participate

All animal experiments were approved by the Animal Ethics committee of Anhui University of Chinese Medicine (Hefei, China).

### Patient consent for publication

Not applicable.

## Competing interests

The authors declare that they have no competing interests.

## References

- Smolen JS, Aletaha D and McInnes IB: Rheumatoid arthritis. *Lancet* 388: 2023-2038, 2016.
- Ham S, Bae JB, Lee S, Kim BJ, Han BG, Kwok SK and Roh TY: Epigenetic analysis in rheumatoid arthritis synoviocytes. *Exp Mol Med* 51: 1-13, 2019.
- Li X, Yuan K, Zhu Q, Lu Q, Jiang H, Zhu M, Huang G and Xu A: Andrographolide ameliorates rheumatoid arthritis by regulating the apoptosis-NEtosis balance of neutrophils. *Int J Mol Sci* 20: 5035, 2019.
- Blunk I, Thomsen H, Reinsch N, Mayer M, Försti A, Sundquist J, Sundquist K and Hemminki K: Genomic imprinting analyses identify maternal effects as a cause of phenotypic variability in type 1 diabetes and rheumatoid arthritis. *Sci Rep* 10: 11562, 2020.
- Mameli G, Erre GL, Caggiu E, Mura S, Cossu D, Bo M, Cadoni ML, Piras A, Mundula N, Colombo E, *et al*: Identification of a HERV-K env surface peptide highly recognized in rheumatoid arthritis (RA) patients: A cross-sectional case-control study. *Clin Exp Immunol* 189: 127-131, 2017.
- Muschter D, Schäfer N, Stangl H, Straub RH and Grässel S: Sympathetic neurotransmitters modulate osteoclastogenesis and osteoclast activity in the context of collagen-induced arthritis. *PLoS One* 10: e0139726, 2015.
- Lowin T, Annsar TM, Bäuml M, Classen T, Schneider M and Pongratz G: Positive and negative cooperativity of TNF and B cell survival in fibroblast/B cell co-cultures. *Sci Rep* 10: 780, 2020.
- Zhao J, Chen B, Peng X, Wang C, Wang K, Han F and Xu J: Quercetin suppresses migration and invasion by targeting miR-146a/GATA6 axis in fibroblast-like synoviocytes of rheumatoid arthritis. *Immunopharmacol Immunotoxicol* 42: 221-227, 2020.
- Lucchino B, Spinelli FR, Iannuccelli C, Guzzo MP, Conti F and Di Franco M: Mucosa-environment interactions in the pathogenesis of rheumatoid arthritis. *Cells* 8: 700, 2019.
- Cappelli LC, Thomas MA, Bingham CO III, Shah AA and Darrach E: Immune checkpoint inhibitor-induced inflammatory arthritis as a model of autoimmune arthritis. *Immunol Rev* 294: 106-123, 2020.
- Matta R, Wang X, Ge H, Ray W, Nelin LD and Liu Y: Triptolide induces anti-inflammatory cellular responses. *Am J Transl Res* 1: 267-282, 2009.
- Guo Q, Mao X, Zhang Y, Meng S, Xi Y, Ding Y, Zhang X, Dai Y, Liu X, Wang C, *et al*: Guizhi-Shaoyao-Zhimu decoction attenuates rheumatoid arthritis partially by reversing inflammation-immune system imbalance. *J Transl Med* 14: 165, 2016.
- Liu XY, Xu L, Wang Y, Li JX, Zhang Y, Zhang C, Wang SS and Zhang XM: Protective effects of total flavonoids of astragalus against adjuvant-induced arthritis in rats by regulating OPG/RANKL/NF- $\kappa$ B pathway. *Int Immunopharmacol* 44: 105-114, 2017.
- Pu X, Ma X, Liu L, Ren J, Li H, Li X, Yu S, Zhang W and Fan W: Structural characterization and antioxidant activity in vitro of polysaccharides from angelica and astragalus. *Carbohydr Polym* 137: 154-164, 2016.
- Dong Z, Zhao P, Xu M, Zhang C, Guo W, Chen H, Tian J, Wei H, Lu R and Cao T: Astragaloside IV alleviates heart failure via activating PPAR $\alpha$  to switch glycolysis to fatty acid  $\beta$ -oxidation. *Sci Rep* 7: 2691, 2017.
- Chen L, Xie ZY, Liu L, Zhu L, Wang F, Fan P, Sinkemani A, Zhang C, Hong X and Wu XT: Nuclear factor-kappa B-dependent X-box binding protein 1 signalling promotes the proliferation of nucleus pulposus cells under tumour necrosis factor alpha stimulation. *Cell Prolif* 52: e12542, 2019.
- Chen X, Chen X, Gao J, Yang H, Duan Y, Feng Y, He X, Gong X, Wang H, Wu X and Chang J: Astragaloside III enhances anti-tumor response of NK cells by elevating NKG2D and IFN- $\gamma$ . *Front Pharmacol* 10: 898, 2019.
- Jiang H, Wu FR, Liu J, Qin XJ, Jiang NN and Li WP: Effect of astragalosides on long non-coding RNA expression profiles in rats with adjuvant-induced arthritis. *Int J Mol Med* 44: 1344-1356, 2019.
- Xu F, Jin L, Jin Y, Nie Z and Zheng H: Long noncoding RNAs in autoimmune diseases. *J Biomed Mater Res A* 107: 468-475, 2019.
- Zhang TP, Zhu BQ, Tao SS, Fan YG, Li XM, Pan HF and Ye DQ: Long non-coding RNAs genes polymorphisms and their expression levels in patients with rheumatoid arthritis. *Front Immunol* 10: 2529, 2019.
- Jiang H, Liu J, Fan C, Wang J and Li W: lncRNAS56464.1 as a ceRNA promotes the proliferation of fibroblast-like synoviocytes in experimental arthritis via the Wnt signaling pathway and sponges miR-152-3p. *Int J Mol Med* 47: 17, 2021.
- Bi X, Guo XH, Mo BY, Wang ML, Luo XQ, Chen YX, Liu F, Olsen N, Pan YF and Zheng SG: LncRNA PICSAR promotes cell proliferation, migration and invasion of fibroblast-like synoviocytes by sponging miRNA-4701-5p in rheumatoid arthritis. *EBioMedicine* 50: 408-420, 2019.
- Jiang H, Qin XJ, Li WP, Ma R, Wang T and Li ZQ: LncRNAs expression in adjuvant-induced arthritis rats reveals the potential role of LncRNAs contributing to rheumatoid arthritis pathogenesis. *Gene* 593: 131-142, 2016.
- Fan C, Cui X, Chen S, Huang S and Jiang H: LncRNA LOC100912373 modulates PDK1 expression by sponging miR-17-5p to promote the proliferation of fibroblast-like synoviocytes in rheumatoid arthritis. *Am J Transl Res* 12: 7709-7723, 2020.
- Jiang H, Liu J, Wang T, Gao JR, Sun Y, Huang CB, Meng M and Qin XJ: Urinary metabolite profiling provides potential differentiation to explore the mechanisms of adjuvant-induced arthritis in rats. *Biomed Chromatogr* 30: 1397-1405, 2016.
- Zhu L, Li J, Guo L, Yu X, Wu D, Luo L, Zhu L, Chen W, Chen C, Ye C and Zhang D: Activation of NALP1 inflammasomes in rats with adjuvant arthritis; a novel therapeutic target of carboxyamidotriazole in a model of rheumatoid arthritis. *Br J Pharmacol* 172: 3446-3459, 2015.
- Luo C, Liang JS, Gong J, Zhang HL, Feng ZJ, Yang HT, Zhang HB and Kong QH: miRNA-31 over-expression improve synovial cells apoptosis induced by RA. *Bratisl Lek Listy* 119: 355-360, 2018.
- Chen L, Feng L, Wang X, Du J, Chen Y, Yang W, Zhou C, Cheng L, Shen Y, Fang S, *et al*: Mesencephalic astrocyte-derived neurotrophic factor is involved in inflammation by negatively regulating the NF- $\kappa$ B pathway. *Sci Rep* 5: 8133, 2015.
- Livak KJ and Schmittgen TD: Analysis of relative gene expression data using real-time quantitative PCR and the 2(-Delta Delta C(T)) method. *Methods* 25: 402-408, 2001.
- Yang Y, Dong Q and Li R: Matrine induces the apoptosis of fibroblast-like synoviocytes derived from rats with collagen-induced arthritis by suppressing the activation of the JAK/STAT signaling pathway. *Int J Mol Med* 39: 307-316, 2017.
- Siu MKY, Jiang YX, Wang JJ, Leung THY, Ngu SF, Cheung ANY, Ngan HYS and Chan KKL: PDK1 promotes ovarian cancer metastasis by modulating tumor-mesothelial adhesion, invasion, and angiogenesis via  $\alpha$ 5 $\beta$ 1 integrin and JNK/IL-8 signaling. *Oncogenesis* 9: 24, 2020.
- He J, Wang Y, Liu T, Liu G, Chen S, Li Q, Quan Y, Yang H, Feng J, Wang S, *et al*: Stage-specific requirement of kinase PDK1 for NK cells development and activation. *Cell Death Differ* 26: 1918-1928, 2019.
- Song X, Wang Z, Liang H, Zhang W, Ye Y, Li H, Hu Y, Zhang Y, Weng H, Lu J, *et al*: Dioscin induces gallbladder cancer apoptosis by inhibiting ROS-mediated PI3K/AKT signalling. *Int J Biol Sci* 13: 782-793, 2017.
- Saji M, Kim CS, Wang C, Zhang X, Khanal T, Coombes K, La Perle K, Cheng SY, Tschlis PN and Ringel MD: Akt isoform-specific effects on thyroid cancer development and progression in a murine thyroid cancer model. *Sci Rep* 10: 18316, 2020.
- Bunte K and Beikler T: Th17 cells and the IL-23/IL-17 axis in the pathogenesis of periodontitis and immune-mediated inflammatory diseases. *Int J Mol Sci* 20: 3394, 2019.
- Bodkhe R, Balakrishnan B and Taneja V: The role of microbiome in rheumatoid arthritis treatment. *Ther Adv Musculoskelet Dis* 11: 1759720X19844632, 2019.
- Wang Y, Zhou J, Tang C, Yu J, Zhu W, Guo J and Wang Y: Positive effect of astragaloside IV on neurite outgrowth via talin-dependent integrin signaling and microfilament force. *J Cell Physiol* 236: 2156-2168, 2021.
- Li N, Wu K, Feng F, Wang L, Zhou X and Wang W: Astragaloside IV alleviates silica-induced pulmonary fibrosis via inactivation of the TGF- $\beta$ 1/Smad2/3 signaling pathway. *Int J Mol Med* 47: 16, 2021.

39. Wang B and Chen MZ: Astragaloside IV possesses anti-arthritis effect by preventing interleukin 1 $\beta$ -induced joint inflammation and cartilage damage. *Arch Pharm Res* 37: 793-802, 2014.
40. Wang S, Zuo S, Liu Z, Ji X, Yao Z and Wang X: Study on the efficacy and mechanism of triptolide on treating TNF transgenic mice with rheumatoid arthritis. *Biomed Pharmacother* 106: 813-820, 2018.
41. Xie YF, Feng WW, Liu MC, Xie J, Yu L, Gong XH, Li YX and Peng C: Investigation of efficacy enhancing and toxicity reducing mechanism of combination of aconiti lateralis radix praeparata and paeoniae radix alba in adjuvant-induced arthritis rats by metabolomics. *Evid Based Complement Alternat Med* 2019: 9864841, 2019.
42. Jia Q, Wang T, Wang X, Xu H, Liu Y, Wang Y, Shi Q and Liang Q: Astragalins suppresses inflammatory responses and bone destruction in mice with collagen-induced arthritis and in human fibroblast-like synoviocytes. *Front Pharmacol* 10: 94, 2019.
43. Yan MM, Chen CY, Zhao BS, Zu YG, Fu YJ, Liu W and Efferth T: Enhanced extraction of astragalosides from radix astragali by negative pressure cavitation-accelerated enzyme pretreatment. *Bioresour Technol* 101: 7462-7471, 2010.
44. Salmena L, Poliseno L, Tay Y, Kats L and Pandolfi PP: A ceRNA hypothesis: The rosetta stone of a hidden RNA language? *Cell* 146: 353-358, 2011.
45. Zhao CC, Jiao Y, Zhang YY, Ning J, Zhang YR, Xu J, Wei W and Kang-Sheng G: Lnc SMAD5-AS1 as ceRNA inhibit proliferation of diffuse large B cell lymphoma via Wnt/ $\beta$ -catenin pathway by sponging miR-135b-5p to elevate expression of APC. *Cell Death Dis* 10: 252, 2019.
46. Mo BY, Guo XH, Yang MR, Liu F, Bi X, Liu Y, Fang LK, Luo XQ, Wang J, Bellanti JA, *et al*: Long non-coding RNA GAPLINC promotes tumor-like biologic behaviors of fibroblast-like synoviocytes as MicroRNA sponging in rheumatoid arthritis patients. *Front Immunol* 9: 702, 2018.
47. Yan S, Wang P, Wang J, Yang J, Lu H, Jin C, Cheng M and Xu D: Long non-coding RNA HIX003209 promotes inflammation by sponging miR-6089 via TLR4/NF- $\kappa$ B signaling pathway in rheumatoid arthritis. *Front Immunol* 10: 2218, 2019.
48. Li G, Liu Y, Meng F, Xia Z, Wu X, Fang Y, Zhang C, Zhang Y and Liu D: LncRNA MEG3 inhibits rheumatoid arthritis through miR-141 and inactivation of AKT/mTOR signalling pathway. *J Cell Mol Med* 23: 7116-7120, 2019.
49. Sun L, Tu J, Liu C, Pan A, Xia X and Chen X: Analysis of lncRNA expression profiles by sequencing reveals that lnc-AL928768.3 and lnc-AC091493.1 are novel biomarkers for disease risk and activity of rheumatoid arthritis. *Inflammopharmacology* 28: 437-450, 2020.
50. Sun C, Sun Y, Jiang D, Bao G, Zhu X, Xu D, Wang Y and Cui Z: PDK1 promotes the inflammatory progress of fibroblast-like synoviocytes by phosphorylating RSK2. *Cell Immunol* 315: 27-33, 2017.
51. Xu H, He Y, Yang X, Liang L, Zhan Z, Ye Y, Yang X, Lian F and Sun L: Anti-malarial agent artesunate inhibits TNF-alpha-induced production of proinflammatory cytokines via inhibition of NF-kappaB and PI3 kinase/Akt signal pathway in human rheumatoid arthritis fibroblast-like synoviocytes. *Rheumatology (Oxford)* 46: 920-926, 2007.
52. Ichikawa R, Kawasaki R, Iwata A, Otani S, Nishio E, Nomura H and Fujii T: MicroRNA-126-3p suppresses HeLa cell proliferation, migration and invasion, and increases apoptosis via the PI3K/PDK1/AKT pathway. *Oncol Rep* 43: 1300-1308, 2020.
53. Shen X, Yu Y, Ma P, Luo Z, Hu Y, Li M, He Y, Zhang Y, Peng Z, Song G and Cai K: Titanium nanotubes promote osteogenesis via mediating crosstalk between macrophages and MSCs under oxidative stress. *Colloids Surf B Biointerfaces* 180: 39-48, 2019.
54. Chen D, Zeng S, Huang M, Xu H, Liang L and Yang X: Role of protein arginine methyltransferase 5 in inflammation and migration of fibroblast-like synoviocytes in rheumatoid arthritis. *J Cell Mol Med* 21: 781-790, 2017.
55. Fu H, Zhang W, Yuan Q, Niu M, Zhou F, Qiu Q, Mao G, Wang H, Wen L, Sun M, *et al*: PAK1 promotes the proliferation and inhibits apoptosis of human spermatogonial stem cells via PDK1/KDR/ZNF367 and ERK1/2 and AKT pathways. *Mol Ther Nucleic Acids* 12: 769-786, 2018.



This work is licensed under a Creative Commons Attribution-NonCommercial-NoDerivatives 4.0 International (CC BY-NC-ND 4.0) License.